Combined heat and power operational modes for increased product flexibility in a waste incineration plant

Citation for the original published paper (version of record):
Beiron, J., Mocholí Montañés, R., Normann, F. et al (2020). Combined heat and power operational modes for increased product flexibility in a waste incineration plant. Energy, 202. http://dx.doi.org/10.1016/j.energy.2020.117696

(article starts on next page)

Combined heat and power operational modes for increased product flexibility in a waste incineration plant

Johanna Beiron*, Rubén M. Montañés, Fredrik Normann, Filip Johnsson

Department of Space, Earth and Environment, Chalmers University of Technology, S-412 96 Göteborg, Sweden

*Corresponding author
E-mail address: beiron@chalmers.se

Link to published article: https://doi.org/10.1016/j.energy.2020.117696

Published in Energy, article number 117696

Abstract

The expected strong expansion of wind power may cause challenges for the electricity system in terms of grid stability, power balance, and increased electricity price volatility. This paper analyses how the new market conditions impact the operational pattern and revenue of a combined heat and power (CHP) plant. The work focuses on product flexibility that enables varied ratios between products; and thermal flexibility, to shift load in time given the differing timescales of heat and power demand. Product flexibility is given by five operational modes: conventional CHP, heat-only, CHP plus frequency response, condensing, and condensing plus frequency response. Optimization and process modeling are combined to study the plant dispatch in current and future electricity market scenarios and with thermal flexibility. The results indicate that load-shifting of heat generation together with condensing operation can increase revenue up to 4.5 M€ and plant utilization up to 100% for a 50 MW_{el} waste-fired plant; but requires a thermal energy storage to meet hourly heat demand. The electricity price profile impacts both the revenue and operational patterns, with low-price periods favoring increased heat generation and frequency response delivery. High average electricity price and price volatility results in increased profitability of product and thermal flexibility.

Keywords: Combined heat and power; District heating; Thermal power plant; Operational flexibility; Optimization model; Thermal energy storage

1. Introduction

The share of non-dispatchable power generation is increasing rapidly in many European energy systems as a strategy to mitigate climate change [1]. The focus region of this work is Northern Europe, where wind power, in particular, is expected to become a major energy source in future energy systems. Large shares of wind power in electricity systems with limited flexibility will lead to lower electricity prices, due to the low operational costs, but also to price volatility, due to the non-dispatchability of wind; and, possibly, to issues related to power system vulnerability and reduced inertia [2]. One way to balance the variability of wind power generation is dispatching of controllable power generating units in the system, e.g. thermal power plants. Other variation management strategies to increase the system flexibility include: batteries, demand side response or transmission to neighboring systems. For thermal power generating units to balance the power system, it will be of importance to apply new modes of operation to maintain profitability from participating in the energy markets, while also being available as dispatchable power generation capacity in the electricity system.

Increasing the flexibility of thermal power plants could be an opportunity to enhance profitability of operation. For condensing plants, the operational flexibility is centered around the fuel conversion unit; with minimum load level, ramp rate and cycling properties being the main parameters to consider [3,4]. Polygeneration units, such as combined heat and power (CHP) plants that produce electricity and district heating (DH), have additional opportunities for flexibility, with the possibility to vary the ratio between products – product flexibility – [5,6] and to shift load in time given the differing timescales of heat and power [7]. The possibility for an energy system to optimize when to generate heat by implementation of thermal energy storage (TES) for DH has been shown to reduce the primary energy consumption and operating cost of the system [8]. Additionally, polygeneration has been identified as an important part of sustainable and energy efficient systems [9–11].

For steam cycle-based CHP plants, the possibility to vary the power-to-heat ratio; i.e. the product flexibility; lies mainly in the regulation of steam flow to turbine extractions and bypasses. Gao et al. [12] investigated the implementation of a two-stage turbine bypass using a dynamic model of a CHP plant. Wang et al. [13] modeled a control system for flexible operation of an extraction condenser for DH production. Zhao et al. [14] studied how steam extraction regulation to a power plant-internal TES could provide flexible power generation. Thermal energy storages are more commonly found in district heating systems, and may be required to fully utilize the flexibility potential of the differing timescales of heat and power, i.e. to load shift production in time and decouple heat and power generation [15]. There are several types of TES that have been found beneficial for DH network applications, for example: hot water accumulation in tanks [16], utilizing the thermal mass in buildings [17] or in the DH network piping [18].

In addition to the electricity and district heating markets, ancillary markets for power system services, for instance primary frequency response (FCR-N), may present additional market opportunities for CHP plants [19]. Simoglou et al. [20] found that it may occasionally be profitable for thermal power generating units to slightly reduce their electricity generation below the rated maximum in order to contribute to reserve markets, rather than to only produce power for the electricity market. The requirements to participate in ancillary markets differ between countries [21], but previous studies have shown that CHP plants may be able to follow such requirements in Finland [22] and Germany [23]. Lund et al. [24] further argue that the inclusion of CHP plants in sustainable energy systems is important for grid stability when integrating variable renewable energy sources.

Hence, previous works have studied technical solutions that enable thermal power plants to participate in energy markets in a flexible manner; giving rise to a selection of operational modes and strategies that the plant can choose from to prioritize generation of a certain product when market conditions are favorable [25–27]. However, to date, few studies have focused on how technical plant-level flexibility measures interact with system boundary conditions (e.g. market price levels and demands) and impact the operational patterns and profitability of the plant. Thus, there is a need to investigate how technical solutions are dispatched in various market settings, and to give insight into the economic incentives for thermal plant owners to invest in measures that improve flexibility.

This paper focuses on the operation of a heat-driven waste-fired combined heat and power plant in a Nordic setting, and how the operational flexibility of the plant can be enhanced by product flexibility; i.e. implementation of a set of steam cycle operational modes; coupled with thermal flexibility such as from a thermal energy storage. The impact of market scenarios and technical aspects on the operation of the plant is analyzed, with plant revenue and utilization as key performance indicators. Hence, process and system level analyses are combined in the study, approaching a holistic view on the technical and economic potential of combined heat and power flexibility.

2. Method

Figure 1 summarizes the method. The work is centered around an optimization model that cost-optimizes the operation of a waste-fired CHP plant, based on input data for: plant performance and operational range, price for electricity, frequency response and fuel cost, district heating demand and TES capacity. The plant performance is simulated with process models based on a reference plant. The results include the optimal plant dispatch and revenue. The study investigates the potential for flexibility in the CHP plant, and the impact on the optimization model results of variability in the input data. The six variables that are analyzed are:

Technical variables:

- **Product flexibility**. Product flexibility is here defined as the ability to vary electricity generation levels by adjusting product ratios. For the waste-fired plant, the product flexibility lies in the operation of the steam cycle in different modes; with the use of a steam turbine bypass or condensing operation, Section 2.2. With product flexibility, the plant may be operated in five modes with different ratios of electricity, district heating and frequency response. Without product flexibility, the plant generates heat and electricity with a fixed power-to-heat ratio.
- **Thermal flexibility**: Thermal flexibility is here defined as the total flexibility of the district heating system, in terms of MWh of heat that can be stored or load shifted. Here, we consider the implementation of a thermal energy storage, but other measures can also give flexibility to the DH system, e.g. demand side management or dispatch of other heat-generating units. TES sizes analyzed are:
    - 0, no storage.
    - 300 MWh, corresponding to approx. 3 hours of plant heat production, denoted “3h”.
    - 2 500 MWh, approx. 24 hours of heat production, “1d”.
    - 20 000 MWh, 1 week of heat production, “1w”.
- **Mode transition constraint**: For transitions between backpressure and condensing steam cycle modes, an assumed minimum stay-time of a) 1 hour; or b) 10 hours is required before another transition is allowed.

Economic variables:

- **The electricity price profile**. A reference price profile from 2018-19 [28] is compared with generic price profiles and future electricity price scenarios; see Section 2.3.
- **The frequency response price profile**. A reference price profile from 2018-19, $C_{freq,ref}$, [29] is scaled with a factor, f, of a) 0.5, or b) 2, Eq. 1. The scaling is motivated by uncertainty in how frequency response pricing will develop in the future.

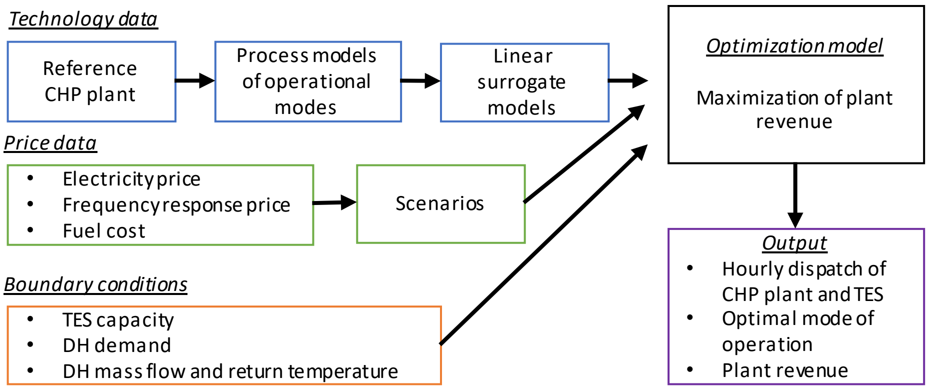

Figure 1. Overview of the methods used in this work, including inputs, outputs and boundaries between models.

$$C_{freq} = C_{freq,ref} \cdot f \qquad (1)$$

- **The fuel cost**. As a base case, the fuel cost for waste is assumed to be 0 €/MWh. Additional cases with 10 and 20 €/MWh fuel costs are compared. An alternative scenario that might have similar implications for the plant would be if, for example, a tax on combustion of waste is introduced, or the plant is subjected to pay CO_2 emission costs.

Note that the heat demand is assumed to be the same regardless of the variations in input data. The combination of process simulation models and optimization modeling enables technical and economic plant performances to be analyzed jointly, rather than separately as is commonly seen in literature. Simplifications of the process simulation models to linear formats (denoted surrogate models in Figure 1) are, however, required for the coupling with the optimization model. Although nonlinearities may be present in the steam cycle part load characteristics, a linear optimization model formulation is chosen to keep the computational complexity low.

2.1 Reference CHP plant

A Swedish 50 MW_{el} waste-fired CHP steam cycle is used as reference for the model development. The plant is operated as a base-load unit in the local municipal district heating system. The circulating fluidized bed boiler is designed for combustion of municipal solid waste, but may also operate with biomass, or co-fire waste and biomass. The boiler load range is 70-100% of maximum load (167 MW fuel). Figure 2 shows the plant configuration with emphasis on the steam cycle. The plant has extraction and backpressure condensers for DH generation (Cond 1-2). Furthermore, there is a turbine bypass (dashed line) connected to a third DH condenser (Cond 3, not in use during regular operation). A thorough plant description is given in [30].

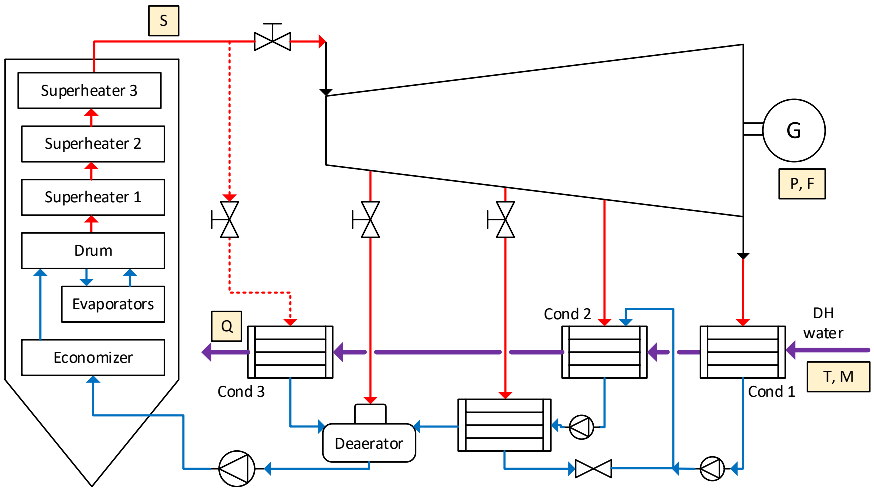

Figure 2. Process schematic of the reference CHP plant. The dashed line indicates an optional steam turbine bypass to condenser 3 (Cond 3). Letters in yellow boxes refer to process variables introduced in Section 2.5.3. Q = the total district heating generation in Cond 1-3. P = electricity generation, F = primary frequency response, S = live steam flow, T = DH return temperature, M = DH mass flow.

2.2 Product flexibility of the steam cycle

Having access to a steam turbine bypass, and the possibility to condense steam with cooling water instead of district heating water, enables plant-level product flexibility with operation in several modes and variable product mix. Five such operational modes are considered in this study:

- **CHP**: Conventional operation, with a fixed ratio of heat and electricity production, not using the steam turbine bypass.
- **HOB**: Operation with full bypass of the steam turbine for heat-only generation.
- **FRQ**: Operation that generates heat, electricity and delivers frequency response services to the power grid, partly using the steam turbine bypass. The ratio between electricity generation and frequency response is fixed with a 25% bypass of the live steam flow.
- **COND**: Condensing operation, with electricity generation only, using cooling water instead of DH water to condense the steam.
- **CFQ**: Condensing operation that delivers frequency response and electricity.

Electricity generation here refers to electricity that is sold on a day-ahead spot market, while frequency response refers to the delivery of primary frequency response that is handled on a separate market [21]. The FRQ and CFQ modes are obtained by adjusting the bypass valve opening for regulation of steam flow to the turbine, i.e. partial steam turbine bypass. Primary frequency response is a symmetrical product in Sweden, and it is assumed that equal amounts of up and down regulation occur over time. On average, the power generation is therefore assumed to be constant, while the instantaneous electricity generation will oscillate. For the hourly timescale considered in this study, the average is used to describe the performance of the FRQ and CFQ modes. Combinations of all five modes could be feasible in practice but are not included in the optimization model.

2.3 Electricity price profiles

Three types of electricity price profiles are considered: a reference price profile for Sweden (price area SE3) between June 2018 – May 2019 (denoted "Ref"); constructed generic price profiles, and scenario profiles obtained from electricity system modeling literature. The generic profiles provide a general analysis of the impact of electricity price volatility on the optimal CHP plant dispatch, while the scenarios are included as a representation of the types of electricity price profiles might be seen under different future scenarios. A volatility index, *VI*, defined as:

$$VI = \frac{\int_{t_1}^{t_2}(price(t) - average\ price)^2\ dt}{t_2 - t_1} \cdot \frac{1}{100} \qquad (2)$$

is introduced as a measure to quantify the price volatility of the profiles.

2.3.1 Generic electricity price profiles

The seven generic price profiles are constructed as step-functions according to Table 1; with the same average electricity price as the reference electricity price profile (49.34 €/MWh), but different price volatility; here expressed with an amplitude that deviates from the average value with a specified duration. A case with constant electricity price is also included. Note that Cases 1-4 have positive prices at all hours, while Cases 5-6 have negative electricity prices during half of the modeling period. The 12 h duration represents diurnal price variations, that might arise from demand variations or variations in solar-dominated electricity systems, while the 168 h (1 week) duration could be representative for wind-dominated systems with slower variations.

Table 1. Characteristics of generic electricity price profiles. The amplitude is the deviation from the average electricity price, 49.34 €/MWh.

Case	Price amplitude, +/- [€/MWh]	Duration [h]	Volatility Index
0	0	6644	0
1	10	12	1
2	10	168	1
3	40	12	16
4	40	168	16
5	80	12	64
6	80	168	64

2.3.2 Electricity price scenarios

The electricity price scenarios consist of price profiles obtained from the electricity system investment model "Hours-to-Decades" (H2D) [31]. The model is semi-heuristic and cost-minimizing, and gives the electricity system generation, transmission and storage capacity for future scenarios with and without flexibility in sector-coupled loads (sectorial collaboration), e.g. electric vehicles [32] or electrified steel-making [33]. Resulting electricity price profiles from the H2D model for the years 2030, 2040, and 2050 are obtained, where the cost of emitting CO_2 is successively increased from 40 €/ton in 2030 to 400 €/ton in 2050 [31]. The geographical price region corresponds to the South of Sweden, but transmission between neighboring regions is included. Thus, six future scenarios are compared, denoted with year and "C" for sectorial collaboration, and "NC" – no collaboration. The electricity price profiles are displayed in the Supplementary material.

Figure 3 plots the average electricity price, number of variations, average duration of variations, and volatility index for the scenario price profiles. The average price decreases from the reference profile to the 2030 profiles, but then increases to 2040 and 2050. For collaboration scenarios (C), the number of variations decreases, while the duration increases. The volatility index ranges from 1.0 to 28.5, where the reference scenario and Cases 1-2 have similar values (1.0), and 2040 scenarios have a price volatility comparable to Cases 3-4 (around 16).

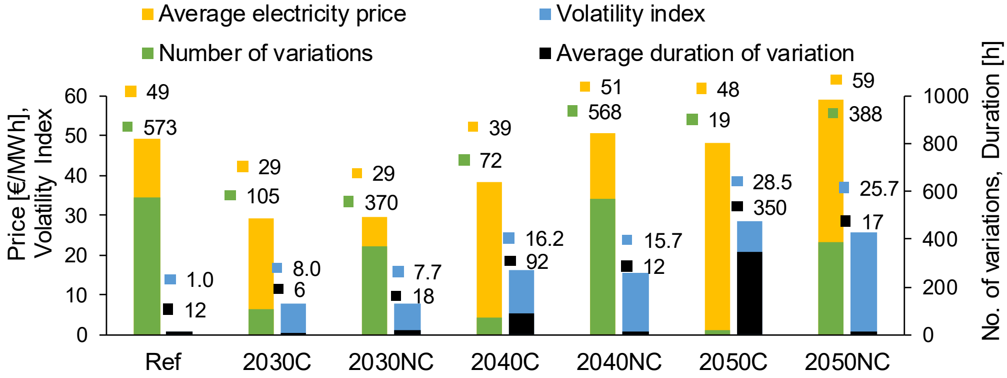

Figure 3. Average electricity price, number of variations, average duration of variations and volatility index for the seven electricity price scenarios. Bars are placed in front of each other, not stacked.

2.4 Optimization model

The mixed integer linear programming optimization model cost-optimizes the CHP plant dispatch. The objective of the model is to maximize the plant revenue for a given heat demand, where income is generated by sales of electricity and frequency response. The plant has to meet the heat demand each hour but may have access to a TES that allows heat generation to deviate from the hourly demand. There is, thus, no price associated with heat production in the objective function, although heat sales will, of course, generate revenue in practice. The decision variables that the model optimizes are: the steam load (representative of the boiler load level) and the optimal mode to operate in. The model is developed using the high-level modeling language GAMS [34] and the formulation is described in detail in the Supplementary material.

Figure 4 presents the network flow model formulation that describes the energy flows and products in the CHP steam cycle. The nodes, S – 8, represent a steam source (S), the five operational modes (1-5) and the three possible products (6-8). The arcs represent energy flows between the nodes. Logical constraints ensure that only one mode can be active during each time step. The plant performance in each mode is given by linear surrogate models derived from process models of the reference CHP plant, as described in Section 2.5. Surrogate process models have been used in optimization models in previous studies, e.g. [35–37].

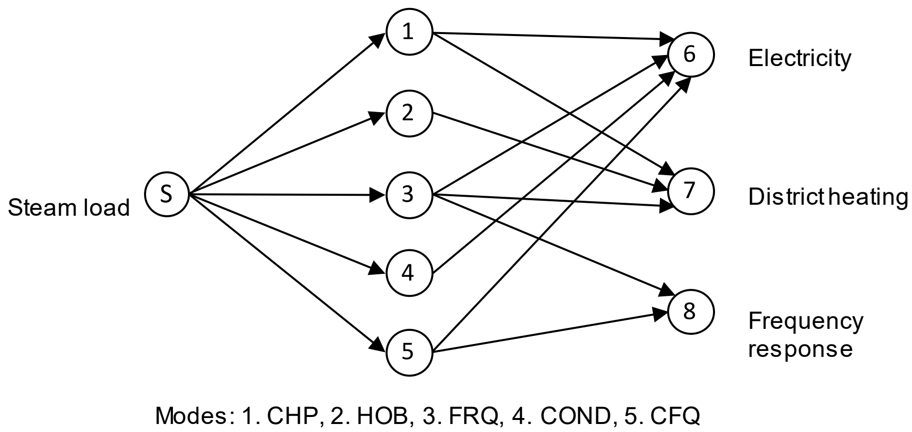

Figure 4. Overview of the optimization model structure.

The modeling time period considered is the plant's heat-generation period from June 2018 – May 2019 with hourly resolution (6644 hours). The model receives input profiles for hourly electricity and frequency response prices; and district heating demand based on the measured reference plant heat production. Fuel and start costs [31] are also specified. Thus, the model has perfect foresight.

Boiler load changes are assumed to be instantaneous and without ramp rate constraints. The same goes for transitions between modes. However, ramp rates have been simulated for the reference CHP plant in previous work using dynamic modeling [30] and should not limit the plant dispatch on an hourly timescale. Plant cycling requires an assumed minimum down time of 144 hours (6 days). Start/stop times are not considered, but optimization modeling of CHP plants with a focus on start/stop procedures is found in [38].

2.5 Surrogate process models

2.5.1 Steady-state process modeling

Stationary process models are developed in the steady-state modeling environment EBSILON Professional [39], based on process and design data from the reference plant. The components used include: a turbine model based on Stodola's law [40]; condensers and a feedwater preheater, a steam generator that evaporates and superheats feedwater to live steam; and condensate and feedwater pumps for flow circulation. The models simulate the steam cycle performance in design and off-design operation for the five modes. Input specifications are given for live steam conditions, turbine nominal extraction pressures, and district heating mass flow and return temperature. The calculated results include the electricity and district heating generation, the steam generator thermal load and process steam parameters.

2.5.2 Steady-state process model validation

The steady-state process model of the CHP mode is validated with reference data for three boiler load levels: 100, 87 and 72% of full load. For each load level, the district heating mass flow and supply and return temperatures are specified inputs, and the electricity generation and steam parameters are calculated outputs. The absolute percentage deviation (AP) of the simulated value (SV) from the reference value (RV) is calculated as:

$$AP = 100\frac{|RV-SV|}{RV} \qquad (3)$$

and given in Table 2 for selected process variables. All simulations are within 5% from the reference values, indicating an adequate fit.

Table 2. Steady-state process model and surrogate model validation results for operation in CHP mode, showing the absolute deviation [%] for selected process variables at three boiler load levels.

Variable	**Reference value**			**Percentage deviation (%)**					
				EBSILON process model			Surrogate model		
Boiler load level (% of full load)	100%	87%	72%	100%	87%	72%	100%	87%	72%
Electricity generation [MW]	48.23	39.64	31.04	2.07	1.33	4.62	2.39	3.01	1.33
District heating generation [MW]	110.90	98.69	82.61	0.26	0.08	0.07	1.83	2.75	3.82
Live steam mass flow [kg/s]	58.47	48.77	40.30	1.14	4.19	4.29	-	-	-
Steam temperature, Cond 2 [°C]	86.35	97.57	95.56	1.59	1.43	1.49	-	-	-
Steam temperature, Cond 1 [°C]	71.55	77.87	77.84	3.43	3.37	3.33	-	-	-

2.5.3 Linearization

The stationary process models are linearized to surrogate models that describe the process performance; i.e. how the electricity, P, and DH, Q, generation and frequency response delivery, F, depend on three factors (marked in Figure 2) that influence the steam cycle performance [41]:

- Live steam flow, S [kg/s]
- DH return temperature, T [°C]
- DH mass flow, M [kg/s]

A 3^3 factorial design is used, with three levels for each factor [42]. The levels are selected based on commonly occurring DH conditions at the reference plant and maximum and minimum steam load. The process models simulate the steam cycle performance for all combinations of levels and the response variables P, Q, and F are computed. Infeasible combinations are excluded. Linear regression determines each factor's effect on the response variables. For each mode, equations on the form presented in Eq. 4 are obtained for P, Q and F. β represents the effect of each factor and y is the response variable. Validation data for the CHP mode surrogate model are presented in Table 2.

$$y = \beta_0 + \beta_S S + \beta_T T + \beta_M M \qquad (4)$$

3. Results and discussion

The results are grouped based on the technical and economic variables analyzed and includes the impact of each variable on the use of operational modes, plant revenue and plant utilization.

3.1 Product flexibility and load range expansion

Figure 5 illustrates the expansion of the plant's feasible load range with the five modes of operation investigated in this work. The modes are indicated by letters: The line A-B marks conventional "CHP" operation with a fixed power-to-heat ratio. D-C represent operation in HOB mode, with heat-only generation. E-F shows the FRQ mode, with a reduced electricity output compared to the CHP mode, in favor of frequency response delivery. The condensing modes are marked by the vertical lines G-H and I-J. Thus, the product flexibility allows the electricity and heat outputs to vary between maximum and minimum levels while the boiler is operated independently on constant load. Compared to nominal production in CHP mode, the maximum feasible electricity and heat output can be increased with 27% and 44%, respectively. The minimum production levels can be reduced by 100%, down to 0 MW.

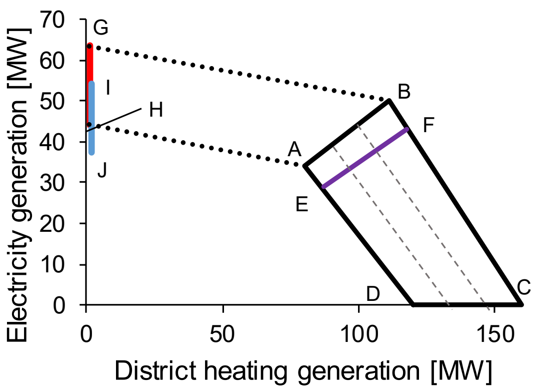

Figure 5. The feasible operating region constituted by the five modes. Backpressure modes are marked by the region A-B-C-D-E-F, while condensing operation is visualized by G-H (COND mode) and I-J (CFQ mode). Dashed lines within A-B-C-D represent operation with constant boiler load. Dotted lines between G-B and H-A indicate transitions between condensing and backpressure modes.

3.2 Utilization of product flexibility

Figure 6 shows the optimal use of steam cycle modes with increasing TES capacity and the reference electricity price profile. Conventional CHP operation without product and thermal flexibilities is represented by the leftmost bar. With product flexibility available, the share of operational hours in CHP mode is reduced to around 70%, in favor of operation in condensing modes (COND + CFQ, 15%) and delivery of frequency response (FRQ, 10-15%). This change is made possible by the thermal flexibility enabled by the TES: since the hourly heat demand must be matched, condensing operation that does not generate heat is not plausible without a TES; and FRQ operation that results in a slightly increased heat generation (Figure 5) is only feasible if the boiler load is reduced, or the excess heat can be stored. The HOB mode is used sparingly, since there is a defined heat demand and no income is granted for excess heat production. The low fuel cost (0 €/MWh) motivates operation in condensing modes, leading to increased revenue. The impact on plant revenue is further analyzed in Section 3.3.2. The optimal use of modes does not change significantly with the TES size; rather, the utilization of the FRQ mode depends on the electricity and frequency price profiles (Section 3.3 and 3.4); while the utilization of condensing modes is limited by the heat demand profile (Section 4).

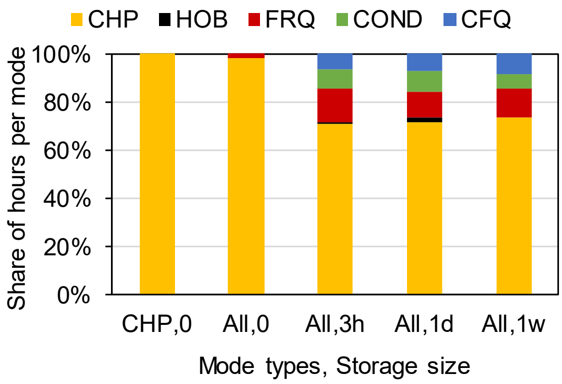

Figure 6. Optimal share of hours spent in each mode when only CHP mode or all modes (product flexibility) are available, with the reference electricity price profile. Different sizes of TES (thermal flexibility) are compared: 0 = no storage, 3h = storage for 3 hours of heat demand, 1d = 1 day (24 hours), and 1w = 1 week's heat demand.

3.3 Impact of electricity price

3.3.1 Generic electricity price profiles

Figure 7 shows the optimal CHP plant mode utilization with the generic electricity price profiles. Thermal flexibility according to a 1w TES size is available in Cases 0-6, while a 1d TES is used in Case "6, 1d". The electricity price volatility impacts the results: with increased volatility the electricity price is at times lower than the frequency response price, or the fuel cost, making different modes more profitable. Compared to Case 0 with constant electricity price ($VI = 0$), the share of, and ratio between CHP/FRQ and COND/CFQ shifts with increasing volatility ($VI = 16$ in Case 4). With $VI = 16$, frequency response delivery is competitive (1) more often during periods with low electricity price (more FRQ, less CHP), and (2) less often during periods with high electricity price (more COND, less CFQ). In Case 6, the even larger volatility ($VI = 64$) yields a negative low-level electricity price, favoring HOB operation, while the high-price periods are spent in COND mode. Figure 8 shows the hourly mode selection for Case 6: the large price volatility results in a bimodal operating strategy where the electricity production pattern resembles that of a peak load plant.

The 1w TES is large enough to cover most of the heat demand during the entire low/high-price periods, be it a 12 or 168 h duration (Table 2), so no significant difference in mode distribution is observed between Cases 1-2, 3-4 and 5-6 (shown in the Supplementary Material). However, if the TES is not large enough to cover the heat demand during a price variation interval, fewer hours are spent in condensing modes (compare Case 6 and Case 6, 1d).

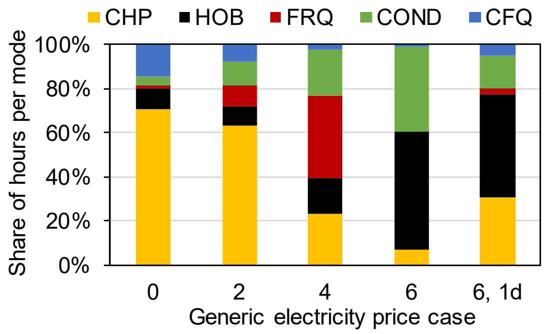

Figure 7. Results for dispatch optimization with generic electricity price profiles. Cases refer to the numbering in Table 2. A 1w TES is used in Cases 0-6, while a 1d TES is used in case "6, 1d".

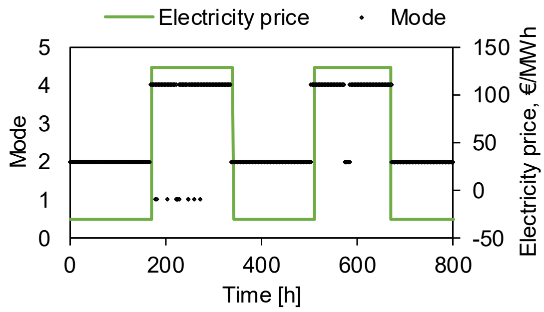

Figure 8. Optimal hourly mode selection for Case 6, over time. The mode selection pattern follows the electricity price profile (green). Modes: 1 = CHP, 2 = HOB, 3 = FRQ, 4 = COND, 5 = CFQ.

3.3.2 Electricity price scenarios

Figure 9 compares the dispatch optimization results for the "collaboration" electricity price scenarios with a 1w TES. The "NC"-scenario distributions are shown in the Supplementary Material and are similar to the "C"-scenarios. The utilization of the FRQ mode increases from around 10% to 30-40% in future scenarios: the increased electricity price volatility causes electricity prices to be lower than frequency response prices more often, favoring frequency response. Heat-only generation is used for 10-20% of operational hours in 2030-2050, to charge the TES for subsequent condensing operation. The distributions of 2030-2050 are similar, indicating that other factors than the electricity price scenario limit further utilization of operational modes, Section 4.

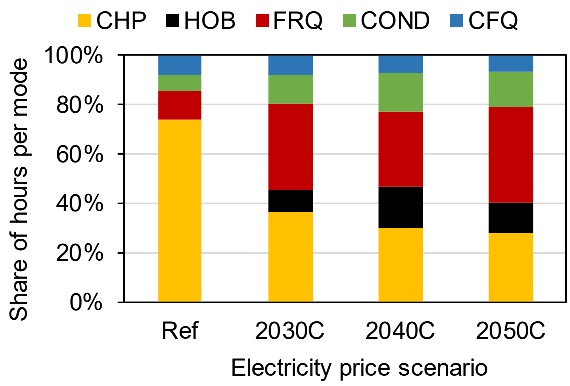

Figure 9. Comparison of optimal shares of hours per mode for different electricity price scenarios. A 1-week TES is used.

Figure 10a plots the increase in annual plant revenue from thermal flexibility in the different electricity price scenarios, for optimal operation in CHP mode only; and Figure 10b gives the additional increase in revenue obtained from operation with product flexibility. The total increase in revenue from both thermal and product flexibility is, thus, given by the sum of the revenue increases in a) and b). For the 50 MW_{el} waste-fired plant, the plant revenue increases with the level of thermal flexibility available, both for operation with and without product flexibility, although the increase is at least twice as large with product flexibility (up to 3 M€) than without (up to 1.5 M€). However, product flexibility does not increase the revenue on its own without thermal flexibility (<0.25 M€). A thermal flexibility of at least 1 000 MWh (corresponding to the order of magnitude of a one-day hot water accumulation tank) is needed for significant impacts on the revenue. Larger heat storage capacities of 10 000 – 100 000 MWh (e.g. a seasonal heat storage) could give benefits in the Year 2040 and 2050 scenarios. Thus, the larger the electricity price volatility (Figure 3), the larger is the economic benefit of thermal flexibility and load-shifting; but the value of product flexibility is independent of the electricity price profile.

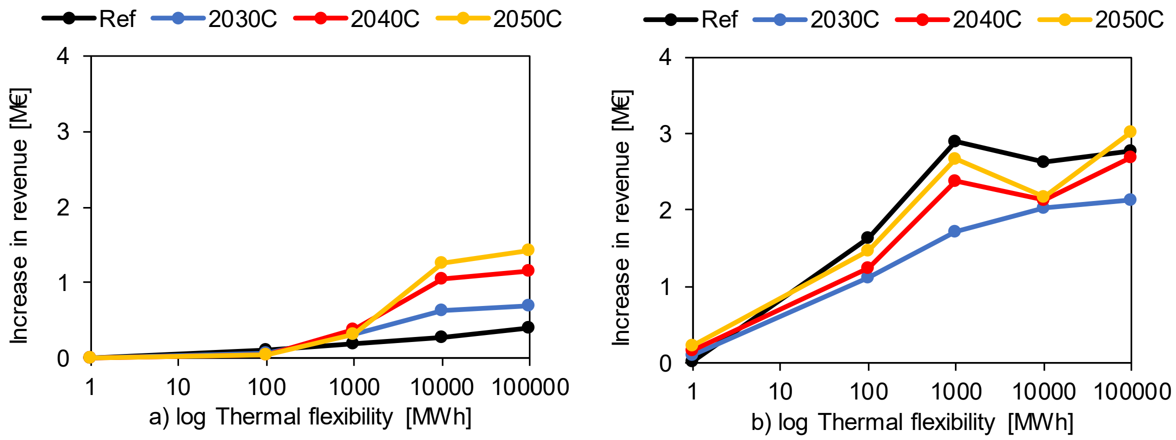

Figure 10. a) The increase in annual plant revenue from thermal flexibility for optimal operation in CHP mode; b) the additional increase in revenue obtained from operation with product flexibility. Different electricity price scenarios are compared. Note the logarithmic scale on the x-axes.

3.4 Impact of frequency response price scaling

Figure 11 shows how the frequency response price level impacts the optimal distribution of hours in each mode, with the reference electricity price profile. Increasing the price level makes frequency response more profitable and shifts operational hours from the CHP and COND modes to FRQ/CFQ modes. The annual plant revenue could thereby increase with 0.25-1.2 M€. The horizontal lines crossing the bars mark the share of the revenue that is gained from offering frequency response, where 15% is reached at a doubling of today's price levels. The remaining share is obtained from electricity sales on the day-ahead market. Thus, even though the share of hours when frequency response is offered approaches 40-45% at the higher price, it is not matched by the gain in revenue. This is largely due to the small volume of frequency response that is delivered from the plant (up to 5 MW) compared to the electricity generation (up to 43 MW in FRQ mode). From a plant perspective, frequency response delivery might therefore not be an objective in itself; but could be considered a byproduct to take advantage of when electricity prices are low.

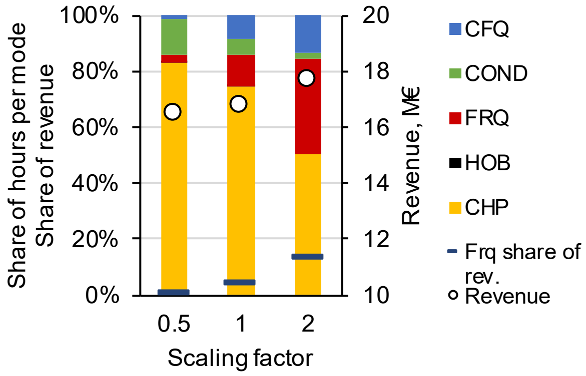

Figure 11. The impact of frequency response price level on optimal mode distribution with the reference electricity price profile. Scaling according to Section 2. TES size: 1d. White dots mark the total revenue from electricity and frequency response sales; horizontal lines mark the share of the revenue that is gained from frequency response delivery.

3.5 Impact of fuel cost

Figure 12 shows how an increased fuel cost (e.g. from an increased fuel tax) impacts the optimal plant operation and revenue. Fuel costs of 0, 10 and 20 €/MWh are compared, for the reference and 2040C electricity price scenarios, with a 1w TES. Obviously, a higher fuel cost lowers the revenue, although a negative revenue does not necessarily mean that plant operation becomes unprofitable, as the income from heat production is not included. For the reference electricity prices, a fuel cost of 10 €/MWh does not affect the plant operation much compared to the zero-cost, while for 20 €/MWh the plant is shut down approximately 7.5% of the modeling time period. For 2040C electricity prices, plant cycling occurs already at 10 €/MWh during 11% of hours, and 17% of hours for the 20 €/MWh fuel cost. Furthermore, an increasing fuel cost leads to more frequent operation in HOB mode (compare 17% for 2040C,0 and 49% for 2040C,20), to maximize the heat production to the lowest fuel input. Additionally, less time is spent in condensing modes, given that heat production is the main priority and a strict plant requirement.

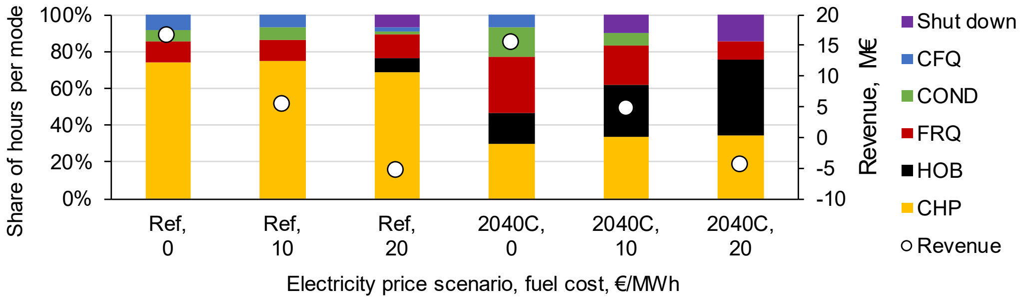

Figure 12. Impact on optimal operation of fuel cost (0, 10 or 20 €/MWh), for a 1w TES and two electricity price scenarios.

3.6 Impact of minimum mode stay-time

If the constraint on minimum mode stay-time (operation for at least 10 hours in the new mode before a switch back is allowed) is added to the model, some freedom of operation is lost, and the possibility to match operational patterns to market conditions is to an extent restricted. However, if a large enough TES is available, adding the minimum stay-time constraint does not impact neither the total revenue nor the mode distribution. Figure 13 gives the optimal mode distributions with and without the constraint on minimum mode stay-time for two TES sizes and the reference electricity price profile. The 3-hour TES does not have enough capacity to supply heat for the entire minimum stay-time; thus, no economic benefit from product or thermal flexibilities is obtained, as condensing modes cannot be used. On the other hand, for the 1d TES, the mode distributions and revenue are similar whether the stay-time constraint is included or not; suggesting that several feasible operating patterns could result in comparable, close to optimal, revenues. An interpretation of this is that the plant has a certain extent of flexibility in choosing the operational pattern, while still maintaining a similar level of revenue.

It can be discussed whether a minimum stay-time constraint should be included for switching to/from the HOB mode, as this would imply a start/stop of the steam turbine that may have an associated minimum time requirement. However, the results indicate that the HOB mode is either used sparingly or in cohesive segments (Figure 8). Thus, adding a minimum time constraint for the use of the HOB mode might not have a significant impact on the results.

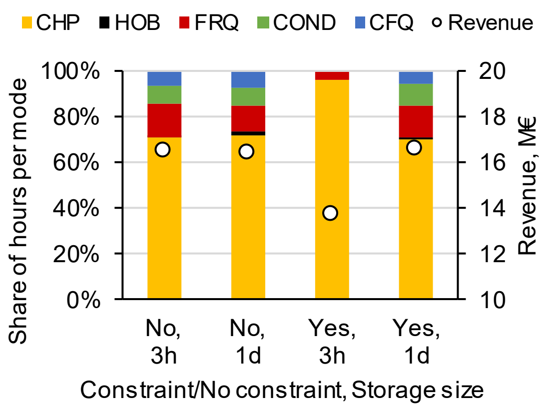

Figure 13. Optimal plant operation with (Yes) and without (No) the 10 h minimum mode stay-time constraint. 2 TES sizes are compared: 3h and 1d.

3.7 Plant utilization and operational patterns

With the TES, opportunities to decouple heat and electricity generation arise. The decoupling will impact the utilization of the plant and its total annual production. Figure 14a shows the optimal boiler operation (steam flow) in the reference scenario where only CHP mode is available, without a TES (conventional operation). The boiler load level is in this case entirely determined by the heat demand; for example, during the low-demand summer period between hours 50-2000, the boiler is operated close to its minimum load level (42 kg/s steam flow). In contrast, Figure 14b shows the optimal boiler operation with a 1d TES. The boiler is now operated at full load for almost the entire modeling period with increased utilization, and instead the TES is cycled to manage heat demand variations. From an operational viewpoint, running the boiler on constant load is preferred, as the thermal stress caused to component metal walls during ramping is minimized. However, the increase in boiler utilization is also partly enabled due to the zero-priced fuel. With a higher fuel cost, the utilization might instead decrease. Figure 14c shows the boiler and TES (1w) dispatch for the 2040C scenario, with a 20 €/MWh fuel cost. Here, more time is spent at the boiler minimum load level, as well as in shut down mode.

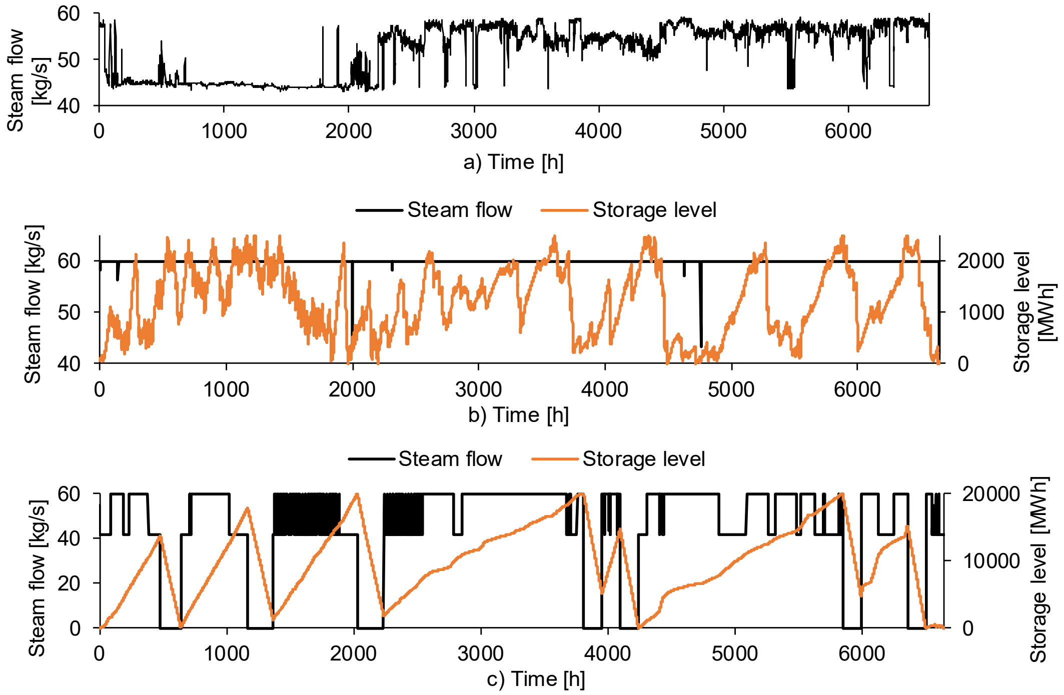

Figure 14. Optimal boiler (steam load) and TES dispatch for a) operation with only the CHP mode available, no TES, and with reference scenario prices; b) all modes available, the reference electricity price profile, and a 1d TES; c) the 2040C electricity price scenario, with fuel cost 20 €/MWh and 1w TES. Note the different scales on the y-axes.

Table 3 presents annual plant production data for two electricity price scenarios, with differing TES capacity and fuel cost. Along with the boiler utilization, or capacity factor, the total revenue and plant production (GWh) increase with storage implementation, although the distribution between electricity and frequency response delivery varies. Less electricity is generated in the 2040C scenario compared to the reference year, even with the TES available, indicating a reduced need for electricity generation from thermal power plants, due to the low-price periods. The heat production is equal for all scenarios, as specified by the model constraints.

Table 3. Annual plant production for two electricity price scenarios, with differing TES capacity (no/1d/1w) and fuel cost.

Case	Ref, CHP only, no TES	Ref, 1d	2040C, 1d	2040C, 1w	2040, 1w, fuel cost 20 €/MWh
Total electricity and frequency response generation [GWh]	292	341.6	332.9	295.1	167.2
Total electricity generation [GWh]	292	334	314	281	164
Total frequency response delivered [GWh]	0	7.6	18.9	14.1	3.2
Boiler capacity factor [-]	0.87	0.99	0.99	0.99	0.74
Total revenue [M€]	13.62	16.42	14.92	15.44	-4.27

4. Practical implications

The results indicate that product and thermal flexibilities can increase the annual revenue of the waste-fired CHP plant; mainly by condensing operation, participation in frequency response markets and load-shifting of heat production to match favorable electricity price periods. However, the maximum share of condensing operation is limited to 20-25% of operational hours independent of electricity price scenario, thermal flexibility or other variables. The upper bound for increased revenue is, instead, defined by the plant's nominal capacity (load range) and role in the district heating system. The waste-fired plant is conventionally operated as base load for heat generation and is dispatched for full load operation a large part of the year (87% utilization as a reference, Table 3), leaving little room for increased production and utilization.

For CHP plants that have higher fuel costs than waste-fired plants (e.g. mid and peak load plants in DH systems), increased utilization might not be economically interesting due to fuel expenses. Rather, heat-only generation and plant cycling is preferable to reduce utilization and operational expenditures, as seen in Figure 12 and Table 3. The operating patterns are, thus, dictated by operating costs, and may be applicable also to other types of thermal cogeneration plants.

In this study, the heat demand profile of the plant is based on conventional operation with a fixed power-to-heat ratio. If product and thermal flexibilities are considered when determining the DH system dispatch, CHP plant operating profiles could be adjusted to provide flexibility to the DH system. For example, excess heat production from the waste-fired plant using the HOB mode could be competitive to the use of expensive peak units, thus lowering the operational cost of the DH system.

Enhancing the product flexibility of the plant and the thermal flexibility of the DH system is beneficial for the plant in all electricity price scenarios, especially for scenarios with high electricity price volatility. Thus, there are synergies between strong price fluctuations and the value of a thermal energy storage. The cost-optimal dimensioning of the TES will depend on several factors including the timescale of price variations. The electricity price variations that dominate the scenarios in this study have long durations (see the electricity price profiles in the Supplementary Material), making a large TES capacity favorable; while smaller sizes could be more appropriate for systems that are dominated by variations occurring with high frequency, e.g. diurnal variations of solar power. However, seeing that investment costs are not included in this study, it is necessary to evaluate the relative gain in revenue from increased flexibility compared to the investment costs of making the required modifications.

5. Conclusion

An assessment of how a waste-fired combined heat and power plant's operation is impacted by the availability of product and thermal flexibilities and market context is performed. The analysis includes five possible modes of operation: conventional CHP, heat-only generation, CHP plus frequency response, condensing, and condensing plus frequency response. An optimization model, with input from a reference plant and process modeling, is developed and determines the most profitable dispatch of the operational modes with regard to the electricity and primary frequency response markets, based on a given demand for district heating. The results include hourly selections for operational mode, plant revenue and utilization. The main conclusions of the study can be summarized by the following points:

- Thermal flexibility is required for the waste-fired CHP plant to benefit from the product flexibility that cogeneration of heat and electricity may provide, as heat generation is the main drive for running the plant.
- The possibility to operate in condensing modes and maximize power generation in periods of high electricity prices, has the largest potential to increase revenue from the operational flexibilities evaluated, although this potential is limited by the requirement on district heating delivery. Frequency response delivery is favored by low electricity prices.
- Product flexibility generally yields a higher plant utilization, unless operational costs increase; in this case cycling of the plant and heat-only generation is preferred by the model to reduce operational expenditures.
- The economic incentives to deliver flexibility using operational modes and thermal energy storages increase with the average electricity price and electricity price volatility index. The plant annual revenue can increase with 1.5-4.5 M€ for a 50 MW_{el} waste-fired CHP plant, depending on the level of thermal flexibility and electricity price scenario.

When serving as base load units in district heating systems, waste-fired cogeneration plants could, thus, provide flexibility and stability to the power and heat sectors, while maintaining plant profitability.

Acknowledgements

This project is financed by the Swedish Energy Agency, Energiforsk – The Swedish Energy Research Centre and Göteborg Energi AB. The authors gratefully acknowledge the support from Mälarenergi AB during the study.

References

[1] European Union. Energy roadmap 2050. 2012. doi:10.2833/10759.

[2] Ciupageanu D-A, Lazaroiu G, Barelli L. Wind energy integration: Variability analysis and power system impact assessment. Energy 2019;185:1183–96. doi:10.1016/j.energy.2019.07.136.

[3] Agora Energiewende. Flexibility in thermal power plants - With a focus on existing coal-fired power plants. 2017.

[4] Ye LC, Lin HX, Tukker A. Future scenarios of variable renewable energies and flexibility requirements for thermal power plants in China. Energy 2019;167:708–14. doi:10.1016/j.energy.2018.10.174.

[5] Anand H, Narang N, Dhillon JS. Unit commitment considering dual-mode combined heat and power generating units using integrated optimization technique. Energy Convers Manag 2018;171:984–1001.

[6] Wang J, You S, Zong Y, Træholt C, Dong ZY, Zhou Y. Flexibility of combined heat and power plants: A review of technologies and operation strategies. Appl Energy 2019;252. doi:10.1016/j.apenergy.2019.113445.

[7] Yao S, Gu W, Zhou S, Lu S, Wu C, Pan G. Hybrid timescale dispatch hierarchy for combined heat and power system considering the thermal inertia of heat sector. IEEE Access 2018;6:63033–44. doi:10.1109/ACCESS.2018.2876718.

[8] Verda V, Colella F. Primary energy savings through thermal storage in district heating networks. Energy 2011;36:4278–86. doi:10.1016/j.energy.2011.04.015.

[9] IEA. Co-generation and Renewables. Solutions for a low-carbon energy future. vol. 1. 2011.

[10] Rong A, Lahdelma R. Role of polygeneration in sustainable energy system development challenges and opportunities from optimization viewpoints. Renew Sustain Energy Rev 2016;53:363–72. doi:10.1016/j.rser.2015.08.060.

[11] Jana K, Ray A, Mansouri M, Assadi M, De S. Polygeneration as a future sustainable energy solution – A comprehensive review. Appl Energy 2017;202:88–111. doi:10.1016/j.apenergy.2017.05.129.

[12] Gao Y, Hu Y, Zeng D, Liu J, Chen F. Modeling and Control of a Combined Heat and Power Unit with Two-Stage Bypass. Energies 2018;11:1395. doi:10.3390/en11061395.

[13] Wang W, Sun Y, Jing S, Zhang W, Cui C. Improved Boiler-Turbine Coordinated Control of CHP Units with Heat Accumulators by Introducing Heat Source Regulation. Energies 2018;11:2815. doi:10.3390/en11102815.

[14] Zhao Y, Wang C, Liu M, Chong D, Yan J. Improving operational flexibility by regulating extraction steam of high-pressure heaters on a 660 MW supercritical coal-fired power plant: A dynamic simulation. Appl Energy 2018;212:1295–309. doi:10.1016/j.apenergy.2018.01.017.

[15] Vandermeulen A, van der Heijde B, Helsen L. Controlling district heating and cooling networks to unlock flexibility: A review. Energy 2018;151:103–15. doi:10.1016/j.energy.2018.03.034.

[16] Mollenhauer E, Christidis A, Tsatsaronis G. Increasing the Flexibility of Combined Heat and Power Plants with Heat Pumps and Thermal Energy Storage. J Energy Resour Technol 2018;140:1–13. doi:10.1115/1.4038461.

[17] Romanchenko D, Kensby J, Odenberger M, Johnsson F. Thermal energy storage in district heating: Centralised storage vs. storage in thermal inertia of buildings. Energy Convers Manag 2018. doi:10.1016/j.enconman.2018.01.068.

[18] Zheng J, Zhou Z, Zhao J, Wang J. Integrated heat and power dispatch truly utilizing thermal inertia of district heating network for wind power integration. Appl Energy 2018;211:865–74. doi:10.1016/j.apenergy.2017.11.080.

[19] Haakana J, Tikka V, Lassila J, Partanen J. Methodology to analyze combined heat and power plant operation considering electricity reserve market opportunities. Energy 2017;127:408–18. doi:10.1016/j.energy.2017.03.134.

[20] Simoglou CK, Biskas PN, Bakirtzis AG. Optimal self-scheduling of a thermal producer in short-term electricity markets by MILP. IEEE Trans Power Syst 2010;25:1965–77. doi:10.1109/TPWRS.2010.2050011.

[21] Montañés RM, Korpås M, Nord LO, Jaehnert S. Identifying operational requirements for flexible CCS power plant in future energy systems. Energy Procedia 2016;86:22–31. doi:10.1016/j.egypro.2016.01.003.

[22] Korpela T, Kaivosoja J, Majanne Y, Laakkonen L, Nurmoranta M, Vilkko M. Utilization of District Heating Networks to Provide Flexibility in CHP Production. Energy Procedia 2017;116:310–9. doi:10.1016/j.egypro.2017.05.077.

[23] Kahlert S, Spliethoff H. Investigation of Different Operation Strategies to Provide Balance Energy With an Industrial Combined Heat and Power Plant Using Dynamic Simulation. J Eng Gas Turbines Power 2016;139:1–8. doi:10.1115/1.4034184.

[24] Lund H, Andersen AN, Østergaard PA, Mathiesen BV, Connolly D. From electricity smart grids to smart energy systems - A market operation based approach and understanding. Energy 2012. doi:10.1016/j.energy.2012.04.003.

[25] Mitra S, Sun L, Grossmann IE. Optimal scheduling of industrial combined heat and power plants under time-sensitive electricity prices. Energy 2013. doi:10.1016/j.energy.2013.02.030.

[26] Mitra S, Grossmann IE, Pinto JM, Arora N. Optimal production planning under time-sensitive electricity prices for continuous power-intensive processes. Comput Chem Eng 2012;38:171–84. doi:10.1016/j.compchemeng.2011.09.019.

[27] Shang C, Srinivasan D, Reindl T. Generation and storage scheduling of combined heat and power. Energy 2017. doi:10.1016/j.energy.2017.02.038.

[28] Nordpool. Historical Market Data 2020. https://www.nordpoolgroup.com/historical-market-data/.

[29] ENTSO-E. Price of Reserved Balancing Reserves 2020. https://transparency.entsoe.eu/balancing/r2/balancingVolumesReservationPrice/show.

[30] Beiron J, Montañés RM, Normann F, Johnsson F. Dynamic modeling for assessment of steam cycle operation in waste-fired combined heat and power plants. Energy Convers Manag 2019;198:111926. doi:10.1016/j.enconman.2019.111926.

[31] Göransson L, Lehtveer M, Nyholm E, Taljegard M, Walter V. The Benefit of Collaboration in the North European Electricity System Transition — System and Sector Perspectives. Energies 2019;12:4648. doi:10.3390/en12244648.

[32] Taljegard M, Göransson L, Odenberger M, Johnsson F. Electric Vehicles as Flexibility Management Strategy for the Electricity System - A Comparison between Different Regions of Europe. Energies 2019;12:2597. doi:10.3390/en12132597.

[33] Vogl V, Åhman M, Nilsson LJ. Assessment of hydrogen direct reduction for fossil-free steelmaking. J Clean Prod 2018. doi:10.1016/j.jclepro.2018.08.279.

[34] GAMS 2020. https://www.gams.com/.

[35] Lythcke-Jørgensen C, Viana A, Münster M. A methodology for designing flexible multi-generation systems. Energy 2016;110:34–54. doi:10.1016/j.energy.2016.01.084.

[36] Andreasen A, Rasmussen KR, Mandø M. Plant Wide Oil and and Gas Separation Plant Optimisation using Response Surface Methodology. Int. Fed. Autom. Control, Elsevier B.V.; 2018, p. 178–84. doi:10.1016/j.ifacol.2018.06.374.

[37] Hansson Björck J, Östlund L. Opportunities for Flexible Operation of a Combined Heat and Power Plant in Power Systems with Volatile Electricity Prices (MSc Thesis). Chalmers University of Technology, 2019.

[38] Weber T, Strobel N, Kohne T, Wolber J, Abele E. Realistic modeling of a combined heat and power plant in the context of mixed integer linear programming. Energy Informatics, vol. 1, 2018, p. 27. doi:10.1186/s42162-018-0037-z.

[39] EBSILON Professional 2020. https://www.steag-systemtechnologies.com/en/products/ebsilon-professional/.

[40] Cooke DH. On Prediction of Off-Design Multistage Turbine Pressures by Stodola's Ellipse. Trans ASME 1985;107:596–606.

[41] Savola T, Keppo I. Off-design simulation and mathematical modeling of small-scale CHP plants at part loads. Appl Therm Eng 2005;25:1219–32. doi:10.1016/j.applthermaleng.2004.08.009.

[42] Montgomery DC. Design and Analysis of Experiments. 5th ed. New York: John Wiley & Sons; 2001.

Combined heat and power operational modes for increased product flexibility in a waste incineration plant

Johanna Beiron, Rubén M. Montañés, Fredrik Normann, Filip Johnsson

Department of Space, Earth and Environment, Chalmers University of Technology, S-412 96 Göteborg, Sweden

Supplementary material

A. Electricity price scenario profiles

The following figures show the electricity price scenario profiles introduced in Section 2.5.1 [1], as well as the reference electricity price profile (Figure 1). The time frame is one year, from January to December.

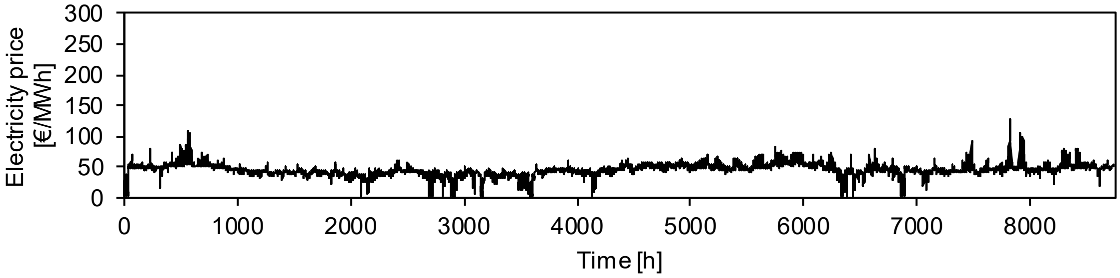

Figure 15. Electricity price profile for the reference time period.

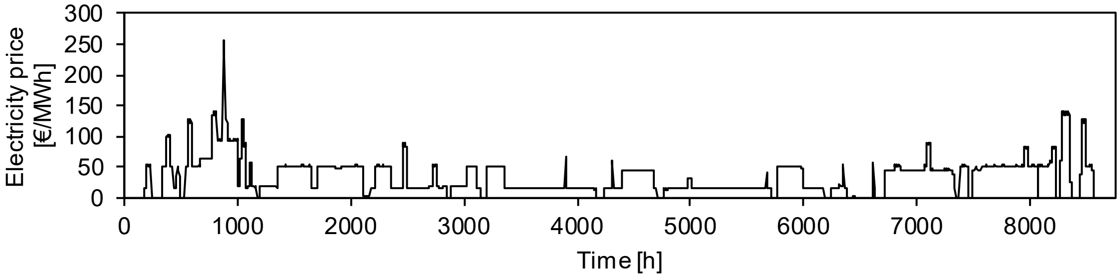

Figure 16. Electricity price profile for the scenario "2030C".

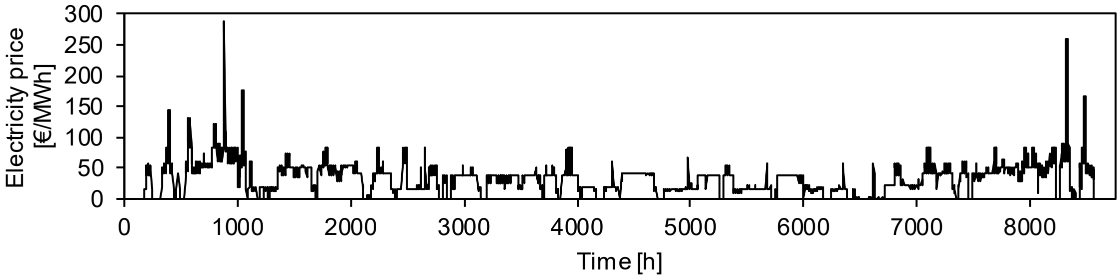

Figure 17. Electricity price profile for the scenario "2030NC".

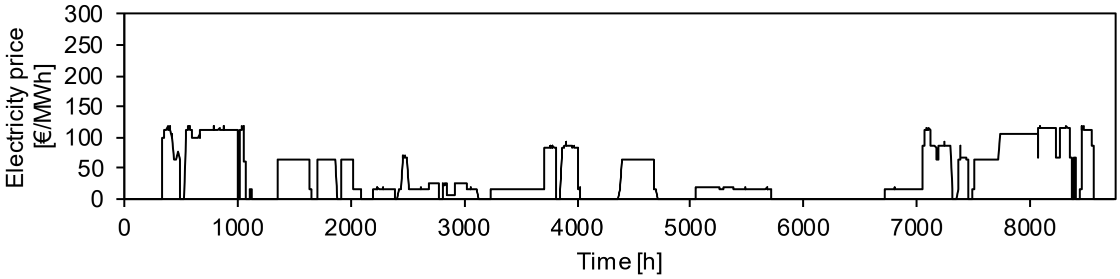

Figure 18. Electricity price profile for the scenario "2040C".

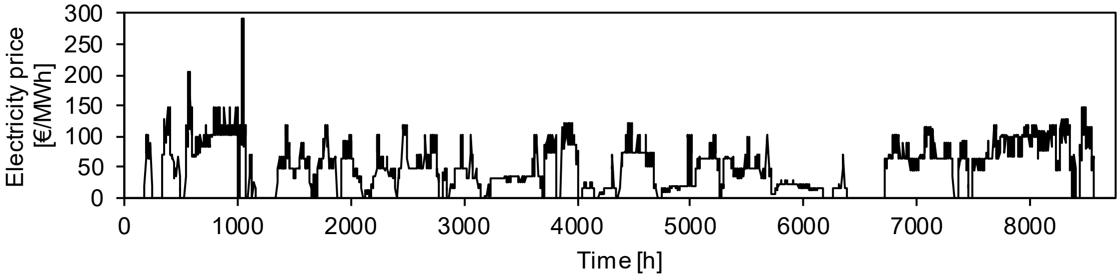

Figure 19. Electricity price profile for the scenario "2040NC".

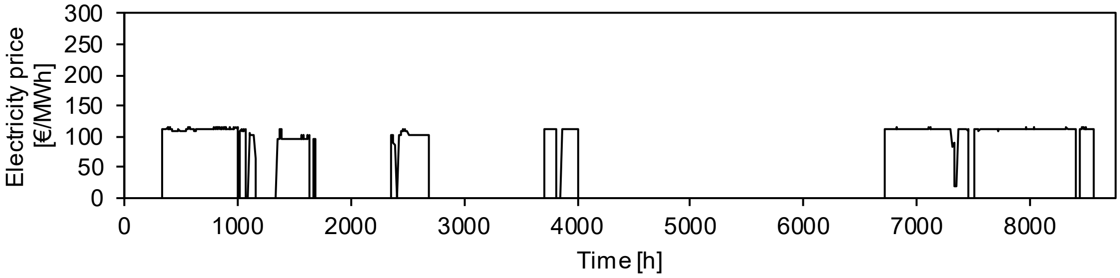

Figure 20. Electricity price profile for the scenario "2050C".

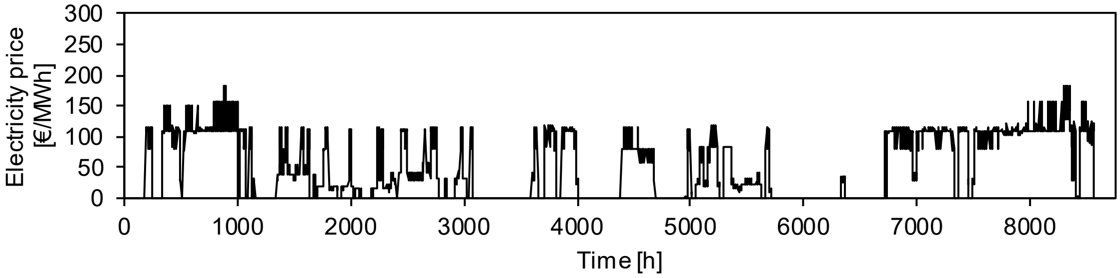

Figure 21. Electricity price profile for the scenario "2050NC".

B. Optimization model formulation

Nomenclature

Sets

t	set of time-steps (hours) in the modeling period
n	set of operational modes
i, j	set of nodes

Parameters

A	total number of time-steps (hours) in the modeling period [-]
S_{max}	maximum steam load [kg/s]
S_{min}	minimum steam load [kg/s]
β	coefficients for linear surrogate models
C_{el}	electricity price at time t [€/MWh]
C_{fuel}	fuel cost [€/MWh]
C_{freq}	frequency response price at time t [€/MWh]
C_{start}	start cost [€/MW]
Q_d	heat demand at time t [MWh/h]
f	scaling factor for frequency response price [-]
L_{max}	installed heat storage capacity/volume [MWh]
M	DH flow rate at time t [kg/s]
T	DH return temperature at time t [°C]
K_s	steam load-boiler load conversion coefficient [MW s/kg]
min_time	minimum mode stay-time [h]
min_off_t	minimum down time of plant cycling [h]
P_{nom}	plant nominal electric capacity [MW]
Q_{minCHP}	minimum heat production in backpressure modes [MWh/h]
M_Q	big M for maximum heat production constraint (B.19) [MWh/h]
M_P	big M for maximum electricity production constraint (B.20) [MWh/h]
dP_s	coefficient relating steam load to maximum electricity production in backpressure mode (B.20) [MWh/h]

Variables

x	energy flow [MWh/h] or steam flow [kg/s], at time t, from node i to node j.
y	binary variable (0,1), 1 if arc from S to mode j is chosen at time t, otherwise 0.
S	Steam load at time t [kg/s]
L	Storage inventory at time t [MWh]
Q_s	heat supplied to DH network [MWh/h]
b	binary variable (0,1), 1 if the unit is operating in mode 1,2, or 3, 0 otherwise
d	binary variable (0,1), 1 if the unit is operating in mode 4 or 5, 0 otherwise
n_{start}	number of plant starts [-]
on123	binary variable (0,1), 1 if a transition to mode 1,2 or 3 from mode 4 or 5 takes place in time step t, 0 otherwise
on45	binary variable (0,1), 1 if a transition to mode 4 or 5 from mode 1,2 or 3 takes place in time step t, 0 otherwise
on	binary variable (0,1), 1 if boiler is started in time step t, 0 otherwise
off	binary variable (0,1), 1 if boiler is shut down in time step t, 0 otherwise
u	binary variable (0,1), 1 if the boiler is in operation at time t, 0 otherwise
z	binary variable (0,1), 1 if the boiler is not in operation at time t, 0 otherwise
sa	steam load, between minimum and maximum load level at time step t [kg/s]
r	revenue, objective function [€]

Objective function

The objective function maximizes the plant revenue, r, from electricity generation and delivery of frequency response, with respect to fuel and start costs. The price for each product is given by an exogeneous input profile with hourly prices and perfect foresight, except for the fuel cost that is assumed to be constant. The parameter K_S correlates the steam flow, S_t, to boiler thermal load, for calculation of the fuel consumption.

$$\max r = \sum_{i=1}^{5}\sum_{t=1}^{A}(C_{el,t}x_{ti6} + C_{freq,t}f(x_{t38} + x_{t58}) - C_{fuel,t}S_tK_S - C_{start}n_{start}P_{nom}) \tag{B.1}$$

Steam load constraints

Eq. B.2-3 constrain the steam load of the plant. B.4 sets the upper limit on energy transfer in the arcs from node S to the mode nodes. If a mode is not selected, the corresponding binary variable y_{tSi} will get the value 0, and as a consequence, no steam can be transferred to this mode from the steam source. B.5 makes sure that all the steam generated at node S is transferred to the mode nodes. B.6 ensures that only one mode can be selected for each time step.

$$S_t = S_{\min}on_t + sa_t \tag{B.2}$$

$$sa_t \leq on_t(S_{max.} - S_{min.}) \tag{B.3}$$

$$x_{tSi} \leq S_{max.}y_{tSi} \tag{B.4}$$

$$S_t = \sum_{i=1}^{5} x_{tSi} \tag{B.5}$$

$$\sum_{i=1}^{5} y_{tSi} = 1 \tag{B.6}$$

Surrogate process model constraints

The plant performance as given by the surrogate process models is expressed by constraints B.7-9, where the linear surrogate model correlations give the power (P) and heat generation (Q) and frequency response (F) provided by each mode, n [MWh/h]. The coefficients for these equations, β, are mode specific (CHP, HOB, FRQ, COND, CFQ).

$$x_{tn6} = x_{t0n}\beta_{S,Pn} + y_{t0n}(\beta_{0,Pn} + \beta_{T,Pn}T_t + \beta_{M,Pn}M_t) \tag{B.7}$$

$$x_{tn7} = x_{t0n}\beta_{S,Qn} + y_{t0n}(\beta_{0,Qn} + \beta_{T,Qn}T_t + \beta_{M,Qn}M_t) \tag{B.8}$$

$$x_{tn8} = x_{t0n}\beta_{S,Fn} + y_{t0n}\beta_{0,Fn} \tag{B.9}$$

Demand-supply constraint

Eq. B.10-11 ensures that the heat supply from the CHP plant (including TES) satisfies the given heat demand at every hour, and that the total heat generation matches the total heat demand for the modeling period. B.12 is a storage inventory balance for the TES, based on heat demand and production at every time step. B.13 ensures that the TES capacity is not exceeded, and B.14 restricts the TES dispatch so that the inventory balance at the start of the modeling time period is the same as the inventory at the end of the period.

$$Q_{s_t} = Q_{d_t} \tag{B.10}$$

$$\sum_{t=1}^{A} Q_{s_t} = \sum_{t=1}^{A} Q_{d_t} \tag{B.11}$$

$$\sum_{i=1}^{3} x_{ti7} = L_t - L_{t-1} + Q_{s_t} \tag{B.12}$$

$$L_t \leq L_{max.} \tag{B.13}$$

$$L_1 = L_{\mathrm{A}} \tag{B.14}$$

Minimum mode stay-time constraints

If a minimum mode stay-time restriction is put on the process, constraints B.15-20 are added to the model. The constraints are adapted from [2]. The binary variables *b, d, on123* and *on45* indicate if the plant is operating in backpressure or condensing mode, and in which time step a transition between these types of modes occur. B.15-16 ensures that the minimum stay-time requirement is met. B.17-18 are logic relations that restricts the plant from operating in both backpressure and condensing modes at the same time. B.19-20 are "big M"-type constraints that limit the power and heat production depending on mode types.

$$\sum_{k=t}^{t+min.\_time-1} b_k \geq on123_t \cdot min.\_time \tag{B.15}$$

$$\sum_{k=t}^{t+min.\_time-1} d_k \geq on45_t \cdot min.\_time \tag{B.16}$$

$$b_t + d_t = 1 \tag{B.17}$$

$$on123_t + on45_t = 1 \tag{B.18}$$

$$\sum_{i=1}^{5} x_{ti7} \leq Q_{minCHP} + M_Q \cdot b_t \tag{B.19}$$

$$\sum_{i=1}^{5} x_{ti6} \leq S_t - dP_S + M_P \cdot d_t \tag{B.20}$$

Plant cycling constraints

The plant cycling constraints are given by B.21-25 (adapted from [2]). The binary variables *u, z,* on_t and off_t allow the boiler to be shut down if operation is not profitable, with a minimum up/down-time *min_off_t*. B.21-22 ensures that the minimum up/down-time requirement is met. B.23-25 are logic equations that make sure that the boiler is, e.g., not started and stopped in the same time step.

$$\sum_{k=t}^{t+min.\_off\_t-1} u_k \geq on_t \cdot min.\_\mathrm{off}\_t \tag{B.21}$$

$$\sum_{k=t}^{t+min.\_off\_t-1} z_k \geq off_t \cdot min.\_\mathrm{off}\_t \tag{B.22}$$

$$u_t + z_t = 1 \tag{B.23}$$

$$on_t + off_t = 1 \tag{B.24}$$

$$on_t - off_t = u_t - u_{t-1} \tag{B.25}$$

C. Additional results

This section presents additional results from the dispatch optimization model, regarding the generic electricity price profiles and future electricity price scenarios, refer to Section 3.3 in the manuscript.

Figure 8 shows the dispatch optimization results for the generic price profiles.

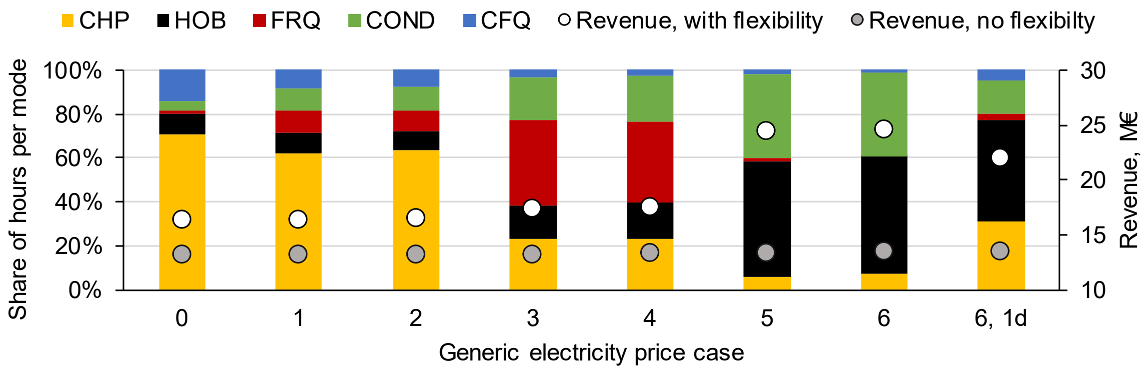

Figure 22. Results for dispatch optimization with generic electricity price profiles. Cases refer to the numbering in Table 2. A 1w TES is used in Cases 0-6, while a 1d TES is used in case "6, 1d". The annual plant revenue is marked by the dots, with thermal and product flexibility (white) and without flexibility (grey).

Figure 9 presents the dispatch optimization results for the future electricity price scenarios.

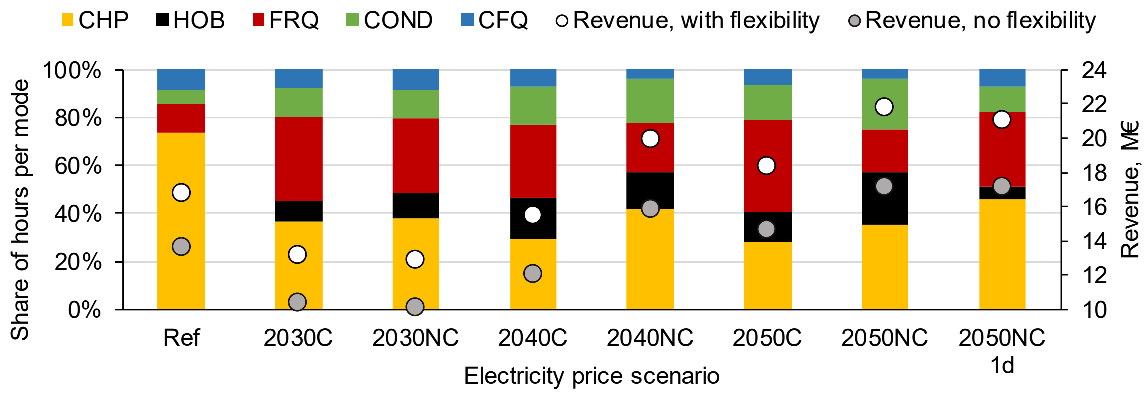

Figure 23. Comparison of optimal shares of hours per mode for different electricity price scenarios. A 1-week TES is used, except for 2050NC 1d, that has a 1d TES. The annual plant revenue is marked by the dots, with thermal and product flexibility (white) and without flexibility (grey).

References

[1] Göransson L, Lehtveer M, Nyholm E, Taljegard M, Walter V. The Benefit of Collaboration in the North European Electricity System Transition — System and Sector Perspectives. Energies 2019;12:4648. doi:10.3390/en12244648.

[2] Romanchenko D, Odenberger M, Göransson L, Johnsson F. Impact of electricity price fluctuations on the operation of district heating systems: A case study of district heating in Göteborg, Sweden. Appl Energy 2017;204:16–30. doi:10.1016/j.apenergy.2017.06.092.